Organic & Biomolecular Chemistry

PAPER

View Article Online
View Journal | View Issue

Cite this: *Org. Biomol. Chem.*, 2015, **13**, 7711

Supramolecular polymers for organocatalysis in water†

Laura N. Neumann, Matthew B. Baker, Christianus M. A. Leenders, Ilja K. Voets, René P. M. Lafleur, Anja R. A. Palmans* and E. W. Meijer*

Received 8th May 2015,
Accepted 9th June 2015

DOI: 10.1039/c5ob00937e

www.rsc.org/obc

A water-soluble benzene-1,3,5-tricarboxamide (BTA) derivative that self-assembles into one-dimensional, helical, supramolecular polymers is functionalised at the periphery with one L-proline moiety. In water, the BTA-derivative forms micrometre long supramolecular polymers, which are stabilised by hydrophobic interactions and directional hydrogen bonds. Furthermore, we co-assemble a catalytically inactive, but structurally similar, BTA with the L-proline functionalised BTA to create co-polymers. This allows us to assess how the density of the L-proline units along the supramolecular polymer affects its activity and selectivity. Both the supramolecular polymers and co-polymers show high activity and selectivity as catalysts for the aldol reaction in water when using *p*-nitrobenzaldehyde and cyclohexanone as the substrates for the aldol reaction. After optimisation of the reaction conditions, a consistent conversion of 92 ± 7%, de_{anti} of 92 ± 3%, and ee_{anti} of 97 ± 1% are obtained with a concentration of L-proline as low as 1 mol%.

Introduction

Catalysts immobilised on soluble macromolecular scaffolds are enjoying renewed interest due to their spatial confinement of catalytic centres, enzyme like-construction, and facile recyclability.[1] However, immobilisation does not always allow exact control over the catalyst localisation on a scaffold, making modulation of the local loading and spatial distance between catalytic sites challenging. A supramolecular approach – the application of reversible, non-covalent interactions – to construct a well-defined macromolecular scaffold has been proposed as a versatile method to control the proximity of catalytic sites.[2] An interesting system to achieve spatial modulation between catalytic sites was demonstrated by Stupp and coworkers. The hydrolysis of a model ester was evaluated using imidazole catalysts attached to the surface of nanofibers formed by aggregation of peptide amphiphiles.[3] A high density of reactive sites on the surface of the ordered supramolecular fibre led to a considerably higher hydrolysis rate than the catalysts in micelles or solution. Moreover, Bouteiller and coworkers reported that helical supramolecular polymers based on a benzene-1,3,5-tricarboxamide (BTA) scaffold with Rh-based catalysts attached to the periphery showed remarkable enantioselectivities for the asymmetric reduction of dimethyl itaconate.[4] The observed selectivity was attributed to the helical bias of the BTA-based polymers. Interestingly, the addition of catalytically inactive BTA-based monomers further enhanced the enantioselectivity of the reduction. These results, along with others,[5] consistently support the observation that spatiotemporal confinement of catalytic centres to a self-assembled structure have consequences for the catalyst activity and selectivity. Additionally, the strength of a supramolecular approach to optimize the catalytic system is demonstrated in these approaches. In a modular fashion, the proximity of catalytic centres and the morphology and nature of the structure can be used to manipulate and optimise the catalytic properties.

L-Proline is a versatile catalyst for a variety of C–C bond forming reactions and is often considered as a mimic for aldolase enzymes;[6] however, in water it is neither an effective nor a selective catalyst.[7] In fact, the first proline derivatives that displayed good activity and selectivity in water contained a hydrophobic fragment.[8] These hydrophobic parts cluster in water, thereby creating hydrophobic pockets in which catalysis occurs. This realisation resulted in many different proline-based catalysts that show high activity and selectivity in water.[9] Recently, we serendipitously found that L-proline attached to the periphery of an organosoluble BTA becomes a highly active and selective organocatalyst for the aldol reaction in water (Scheme 1, L-Pro-BTA).[10] In this system, both hydrophobic interactions and directional hydrogen bonding cooperate to form helical aggregates in water while the introduction of stereogenic centres biases the formation of one type of helical supramolecular polymers, *P* or *M*. However, detailed analysis

Laboratory for Macromolecular and Organic Chemistry, Institute for Complex Molecular Sciences, TU Eindhoven, PO Box 513, 5600 MB Eindhoven, The Netherlands. E-mail: a.palmans@tue.nl, e.w.meijer@tue.nl

†Electronic supplementary information (ESI) available: Details of the experimental procedures and the catalysis experiments. See DOI: 10.1039/c5ob00937e

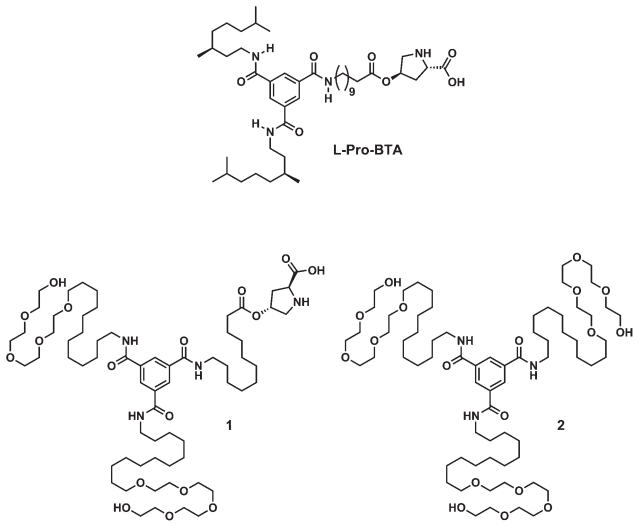

Scheme 1 Molecular structures of BTA derivatives L-**Pro-BTA**, **1** and **2**.

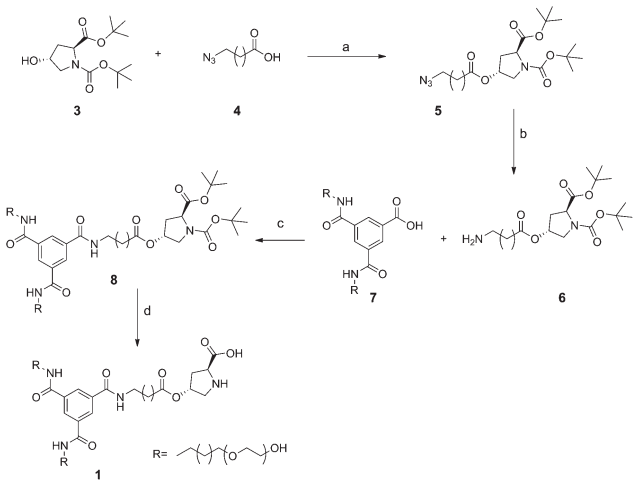

Scheme 2 Reagents and conditions: (a) EDC·HCl, DPTS, $CHCl_3$, r.t., 72 h (59%); (b) PPh_3, H_2O, THF, 35 °C, 72 h (44%); (c) DMT-MM, DMF, r.t., 20 h (35%); (d) TFA, DCM, r.t., 18 h (70%).

of the formed structures suggested that multiple BTA-based helical supramolecular polymers aggregated into less-defined, large assemblies, precluding extensive characterisation.

As a next step in our supramolecular approach towards selective and active catalytic systems in water, we here present an organocatalytic system based on our well-defined, one-dimensional, water-soluble BTA supramolecular polymers.[11] Our aim is to create a system in which we can control the location of the proline units at a hydrophobic/hydrophilic interface and, in addition, tune their density. We here report that BTA **1** (Scheme 1), in analogy to parent BTA **2**, self-assembles in water *via* hydrophobic and hydrogen-bonding interactions, as evidenced by UV-vis and circular dichroism (CD) spectroscopy, small angle X-ray scattering (SAXS), and cryogenic transmission electron microscopy (cryo-TEM). The supramolecular polymers are highly active and selective for the aldol reaction in water. In addition, the density of the proline moieties along the supramolecular polymer is controlled by mixing the system with catalytically inactive BTA **2**.

Results and discussion

Design and synthesis

BTA **1** (Scheme 1) is designed, in analogy to parent BTA **2**, to self-assemble in water *via* hydrophobic and hydrogen-bonding interactions. In two substituents a tetra(ethylene oxide) group is introduced to enhance the water compatibility of BTA **1** compared to L-Pro-BTA. The hydrophobic dodecyl group is required between the central amide groups and the water-soluble part to enable hydrogen-bond formation between the amides of neighbouring BTAs.[11] The third substituent consists of an undecyl spacer coupled to L-hydroxyproline. The undecyl spacer positions the proline unit at the interface of the hydrophobic and hydrophilic domain. Functionalised BTA **1** was obtained in a number of straightforward coupling reactions depicted in Scheme 2. First, protected L-hydroxyproline **3**[12] was coupled to azide-acid **4** to afford azide **5**. Subsequent reduction of **5** resulted in L-hydroxyproline derivative **6**. The ester-amine **6** was unstable and oligomerised slowly over time, even upon storage at low temperatures. Coupling **6** (and its oligomers) to BTA precursor **7**[13] afforded the protected catalytic BTA, **8**. Finally, acid-catalysed deprotection of the *t*-Bu groups yielded compound **1**. Reversed-phase column chromatography in a water/acetonitrile mixture was applied to purify BTA **1** and to remove the fraction which contained the longer spacer resulting from oligomerised **6** (see ESI† for details). BTA **1** was obtained in high purity and moderate yield, as evidenced by NMR, IR and LC-MS (ESI, Fig. S1–S4†). The synthesis and characterisation of BTA **2** has been described previously.[11]

Supramolecular polymerisation of 1 in water

Previously, the supramolecular polymerisation of **2** in water has been studied by a combination of spectroscopic, microscopic and computational methods.[11,18] The combined results showed that compound **2** forms long, one-dimensional supramolecular polymers stabilised by hydrophobic interactions and directional intermolecular hydrogen bonds in water. In contrast to neutral BTA **2**, BTA **1** is zwitterionic in pure water due to the attached L-proline (*trans*-4-hydroxyproline in water: pK_a (acid) = 1.95, pK_a (amine) = 9.47),[14] and the resulting electrostatic perturbation of the molecules may hamper self-assembly into long aggregates.[15] To probe whether screening of the charges by the addition of salt has an influence on the formed structures, the UV–vis absorption was measured in both pure water and phosphate buffered saline (PBS, pH = 7.4). In addition, **1** was measured in methanol, a solvent in which these BTAs are molecularly dissolved (Fig. 1A).

The UV–vis absorption spectrum of **1** in MeOH shows an absorption maximum at 207 nm, indicative for a molecularly

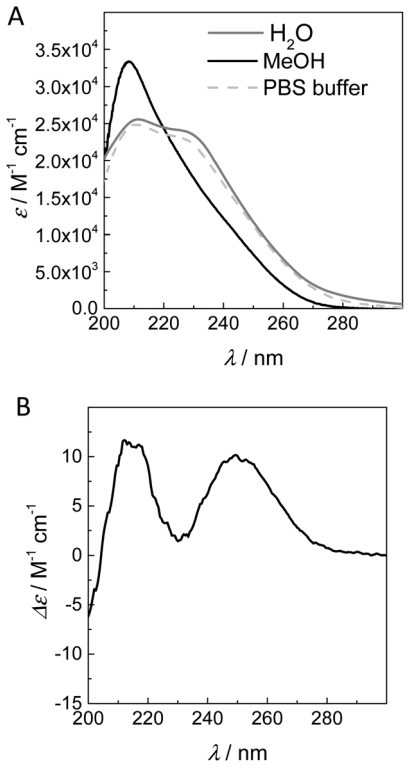

Fig. 1 (A) UV-Vis absorption spectra of **1** in MeOH (black line), water (dark grey line) and PBS buffer (grey dashed line). c = 10 μM in PBS buffer and 50 μM in water and MeOH; (B) CD spectrum of **1** in water. c = 50 μM.

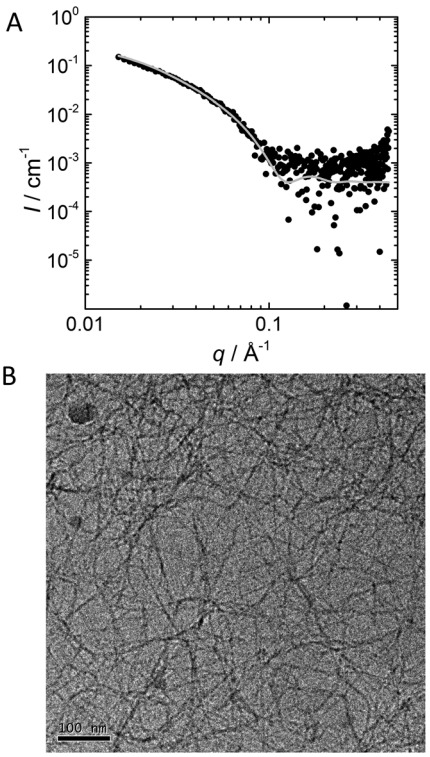

Fig. 2 (A) Experimental SAXS profile of BTA **1**, (c = 3.7 mM in H_2O). The solid grey line is the fit with a form factor model for flexible cylinders (*i.e.*, the Schurtenberger-Pedersen form factor for worm-like, self-avoiding chains).[19] (B) Cryo-TEM image of BTA **1** showing the presence of high aspect ratio fibres (c = 0.4 mM). The dark circular objects in the image are non-vitrified water. The scale bar represents 100 nm.

dissolved state.[16] In contrast, in pure water a peak at 211 nm and shoulder at 226 nm were observed, a spectrum comparable to that previously observed for **2** in its self-assembled state.[11,17] This indicates that **1**, like **2**, forms supramolecular polymers that are stabilised by both hydrophobic interactions and hydrogen bonding in water. In PBS buffer, the UV spectrum of **1** is almost identical to the spectrum measured in water, demonstrating that the charges present on the L-Pro unit in water do not affect the self-assembly behaviour. Since pure water is a simpler solvent system, we decided to perform all remaining experiments using water as solvent. Thus, CD measurements were performed on solutions of **1** in water. We postulated that the stereogenic centres of the L-proline in **1** can bias the helicity of the supramolecular polymers,[18] despite their remoteness from the amides. Satisfyingly, BTA **1** shows a clear CD effect with maxima at 215 and 250 nm (Fig. 1B).

To corroborate the formation of supramolecular polymers by **1** in water, we performed SAXS and cryo-TEM measurements in the high micromolar range. At this concentration, the viscosity of the solution is increased, indicating the formation of sizeable polymeric aggregates. The SAXS profile of **1** (Fig. 2A) shows a q^{-1} decay without a clear plateau, indicative of the presence of long one-dimensional aggregates. A worm-like chain model[19] was selected to fit the data, which assumes an isotropic, semi-flexible cylinder. The fit yields a value for the cross-sectional radius $r_{cs} \sim 3$ nm, while the Kuhn length, L_K – a measure for the stiffness of the polymer – cannot be determined accurately. Thus the data suggests the presence of high-aspect-ratio fibres with a length $L > 40$ nm (the limit of the spectral window).

The aggregates were also visualised with cryo-TEM to confirm the findings from the SAXS measurements. Long, one-dimensional, fibre-like structures formed by self-assembly of **1** can be clearly seen in Fig. 2B. The image suggests that aggregates with lengths in the micrometer range are formed, but it is not possible to extract an exact number for the length of the aggregates. The diameter is estimated at approximately 10 nm. In addition, the fibres entangle and form a network, which is consistent with the observed increase in viscosity at this concentration.

Catalytic activity of the supramolecular polymers in the aldol reaction

None of the techniques discussed above permit to exactly locate the L-Pro units within the supramolecular polymers formed by **1** in water. However, when the organocatalyst is in a sufficiently hydrophobic pocket, active and selective organocatalytic reactions are feasible.[20] Thus, the catalytic activity and selectivity of self-assembled **1** was evaluated using the

model aldol reaction between *p*-nitrobenzaldehyde and cyclohexanone in water. This highly reactive substrate pair is frequently used and allows us to benchmark this system to those reported in literature. In addition, our previously studied **L-Pro-BTA** catalytic system revealed that aldehydes such as *p*-methoxybenzaldehyde were significantly less reactive in the aldol reaction in water.[10] The aldol reaction can yield four stereoisomers, of which the *anti*-(*S*,*R*)-product dominates according to both experimental and computational studies.[21] In addition, we evaluated the activity and selectivity of mixtures (co-polymers) of **1** and catalytically inactive **2**. This "dilution" of **1** within the supramolecular polymers was done to modulate the spatial distribution of the L-Pro units along the polymer chain. Initially, equimolar mixtures of BTA **1** and **2** were prepared. Further dilutions of **1** with **2** were attempted, but in order to keep the catalyst concentration constant, high concentrations of BTA **2** were needed. This caused a significant increase in the viscosity of the catalyst solution, precluding reliable analysis and reproducibility.

To allow comparison with our previous results,[10] the ratio between cyclohexanone and *p*-nitrobenzaldehyde was kept constant at 1 : 10 and an aldehyde concentration of 50 mM was applied. Details for the standard protocol for these experiments are provided in the ESI.† Preliminary screening experiments with **1** and mixtures of **1** and **2** showed excellent selectivities, but the conversions were irreproducible (ESI, Table S1†). We attributed this to poor mixing due to inhomogeneities, as is often the case for organocatalysis in water (ESI, Fig. S5A†). In order to increase the reproducibility, we screened several methods reported in the literature (ESI, Table S1†), most of which were unsatisfactory. Finally, we used a vortex mixer to keep the substrates and products better dispersed during the reaction (Fig. S5B†). This method yielded both near quantitative conversions and an excellent reproducibility of the system; therefore, vortex mixing was used for all subsequent experiments and the results are summarised in Table 1.

We started with a concentration of L-proline ($c_{\text{L-Pro}}$) of 3 mol % (Table 1, entry 1) with respect to *p*-nitrobenzaldehyde. This corresponds to a total BTA concentration (c_{BTA}) of 1.5 mM in the reaction mixture. The conversion was quantitative after 24 h and de_{anti} and ee_{anti} were 87% and 95%, respectively. A 1 : 1 mixture of **1** and **2** ($c_{\text{L-Pro}}$ remains 3 mol% while the BTA concentration, c_{BTA}, doubled to 3 mM) also resulted in a quantitative conversion and a similar selectivity (Table 1, entry 2). Reducing $c_{\text{L-Pro}}$ to 1 mol% (corresponding to a c_{BTA} of 0.5 mM, Table 1, entry 3) gave a quantitative conversion and de_{anti} and ee_{anti} of 85% and 94%, respectively. At this lower catalyst loading, the diastereoselectivity of the reaction slightly improved (91%) by mixing **1** with **2**, while the conversion remained high (92%) (Table 1, entry 4). It should be noted that elimination was not observed in any of these experiments.

The experiment of entry 4 was carried out five additional times under identical conditions to evaluate the reproducibility of the system (Table 1, entry 5). The conversion was constant and high (92 ± 7%) and the selectivities excellent in all cases (de_{anti} = 92 ± 3% and ee_{anti} = 97 ± 1%). To assess whether the supramolecular polymers could be reused, the water layer of entry 4 was purged with argon to remove all volatiles remaining from the extractions. Subsequently, new substrates were added and the reaction was performed under the same conditions. The almost identical results (Table 1, entry 6) indicate that there is no loss of selectivity or activity.

Due to the high activity of the system, the catalyst loading was further decreased to find the minimum catalyst loading required for an active system. At the low loading of 0.2 mol% L-proline, the system still showed excellent activity (conversion = 98 ± 2%, Table 1, entry 7) albeit at the expense of loss in selectivity (de_{anti} = 74 ± 3% and ee_{anti} = 82 ± 3%). To the best of our knowledge, catalyst loadings of 0.2 mol% are among the lowest reported in literature.[22] When decreasing the catalyst concentration even further to 0.1%, a conversion of 37% could still be obtained (Table 1, entry 8), while the selectivity decreased to moderate values. Finally, neither pure BTA **2** nor the mixture of "free" L-Pro mixed with BTA **2** resulted in any aldol product (Table 1, entries 9–10), highlighting that covalent attachment of L-Pro to the supramolecular polymers is crucial to obtain an active catalyst.

Table 1 Aldol reaction catalysed by **1** and equimolar mixtures of **1** and **2**[a]

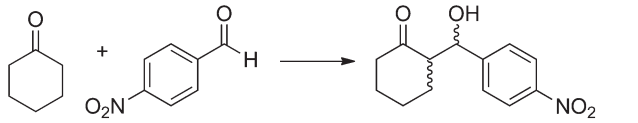

Entry	$c_{\text{L-Pro}}$[b] [mol%]	x_1[c] [mol%]	c_{BTA}[d] [mM]	Conversion[e] [%]	de_{anti}[e] [%]	ee_{anti}[f] [%]
1	3	100	1.5	>99	87	95
2	3	50	3.0	>99	89	97
3	1	100	0.5	>99	85	94
4	1	50	1.0	92	91	96
5[g]	1	50	1.0	92 ± 7	92 ± 3	97 ± 1
6[h]	1	50	1.0	96	93	95
7[i]	0.2	50	0.2	98 ± 2	74 ± 3	82 ± 3
8[i]	0.1	50	0.1	37 ± 5	59 ± 8	50 ± 5
9	0	0	0.5	0	—	—
10	1	0	0.5	0	—	—
11[j]	10	n.a.	n.a.	93	86	96
12[k]	1	n.a.	n.a.	96	98	93
13[l]	1.6	n.a.	n.a.	74	90	71
14[m]	1	n.a.	0.5	>99	90	99

[a] Reaction conditions: reaction volume = 0.5 mL H_2O; aldehyde concentration = 50 mM; substrate ratio (aldehyde : ketone) = 1 : 10; the reactions were carried out at room temperature with a total reaction time of 24 h unless otherwise noted. [b] $c_{\text{L-Pro}}$ is the mol percentage of L-proline relative to the aldehyde. [c] x_1 is the percentage of **1** in mixtures of **1** and **2**. [d] c_{BTA} is the total concentration of BTAs in the mixture. [e] Determined by ^{1}H NMR. [f] Determined by chiral HPLC equipped with a Chiralpak-IA chiral column in hexane/THF 75 : 25, 1 mL min^{-1}. [g] Experiment identical to that in entry 4 but repeated another 5 times to assess reproducibility. [h] Reused solution of entry 4. [i] Reaction time = 52 h, averaged over 2 experiments. [j] Results taken from ref. 23. [k] Results taken from ref. 24*d*. [l] Results taken from ref. 27. [m] Results for L-Pro-BTA taken from ref. 10. n.a. = not applicable.

Discussion

Comparison of the catalysis results of **1** and 1 : 1 mixtures of **1** and **2** with recent literature examples, in which catalysis was performed under similar conditions, reveals that the supramolecular polymers we present here as organocatalysts are highly active and selective for aldol reactions in water. The micellar L-Pro-based aggregates developed by Lipshutz and coworkers showed excellent results, but catalyst loadings below 10 mol% were not reported (Table 1, entry 11).[23] Alternatively, the water-compatible L-Pro-based block copolymers and nanogels prepared by O'Reilly and coworkers are very active and selective, also at low catalyst loadings (Table 1, entry 12).[24] Examples in the literature in which L-proline is attached to oligo(ethylene oxide)-based scaffolds for aldol reactions in water are scarce.[25,26] However, L-Pro attached to a folded amphiphilic PEG containing polymer did show good activity in water, although the selectivity was moderate (ee_{anti} = 72%).[27] This moderate value was attributed to a too hydrophilic environment in the vicinity of the catalyst (Table 1, entry 13). Finally, our previously reported L-Pro-BTA organocatalyst showed very high activities and selectivities, but only after activation of the catalyst with a temperature treatment (Table 1, entry 14).[10]

In BTA **1**, the L-Pro unit is designed to reside at the interface of the hydrophobic aliphatic and hydrophilic tetra(ethylene oxide) parts. While the techniques discussed above do not reveal the exact location of the L-Pro units, the high activity and selectivity in the aldol reaction suggests that a sufficiently hydrophobic pocket is created around the catalytic sites.[20] In addition, the pronounced CD effect shown by **1** suggests a high degree of organisation within the supramolecular polymers, although there is no evidence for additional interactions between the L-Pro units.[10] Moreover, mixing of **1** with **2** does not have a negative effect on the catalytic properties of **1**. Since a lack of mixing between the two BTAs is unlikely based on our experience with BTA-based systems in water,[13,28,29] we conclude that increasing the number of tetra(ethylene oxide)s units, which separate the L-prolines along the supramolecular polymer, does not significantly alter the microenvironment around the catalyst. As a result, changing the local L-proline density on the supramolecular polymer does not negatively affect its activity and selectivity – an observation similar to that made by O'Reilly and coworkers in L-proline-based nanogels.[24]

Our design is successful in positioning L-proline at a well-defined interface between the hydrophobic and hydrophilic portions of the supramolecular polymers, resulting in an active and selective organocatalyst in water. The advantage of BTA **1**, compared to those previously reported by us and others, is that an active, well-characterised and highly reproducible catalyst is easily accessible in preparations at room temperature. As a direct consequence of the stabilisation of the supramolecular polymers in water by both hydrophobic effects and directional hydrogen-bonding interactions, the supramolecular polymers remain intact down to micromolar concentrations.[30] This results in an active system, even at catalyst concentrations as low as 0.1 mol% (50 μM catalyst concentration). In addition, BTA **1** can be easily mixed with structurally related BTAs, which eventually permits to create modular catalytic systems.

Experimental

Materials and methods

All reagents were purchased from Sigma-Aldrich or Acros Organics and used as received, unless otherwise specified. All solvents were purchased from Biosolve. Chloroform and tetrahydrofuran were dried over 4 Å molecular sieves before use. Triethylamine was dried and stored over KOH pellets. Deuterated compounds were obtained from Cambridge Isotopes Laboratories and stored over 4 Å molecular sieves. Reactions were followed by thin-layer chromatography (TLC) using 60-F254 silica gel plates from Merck and visualized by UV light at 254 nm and/or staining (ninhydrin, bromocresol green-, and/or cerium molybdate). Flash column chromatography was performed on a Biotage Isolera II Chromatography system using SNAP columns or a Grace Reveleris X2 system using Grace silica flash cartridges. Reversed phase column chromatography was achieved using a reversed phase KP-C_{18}-HS SNAP column or a Reveleris C18 reversed-phase flash cartridge. (2*S*,4*R*)-Di-*tert*-butyl 4-hydroxypyrrolidine-1,2-dicarboxylate (**3**),[12,31] 3,5-bis((1-hydroxy-3,6,9,12-tetraoxatetracosan-24-yl)carbamoyl)benzoic acid **7**[13] and DMT-MM[32] were synthesized according to literature procedures. Phosphate buffered saline (PBS) tablets were obtained from Aldrich. One tablet was dissolved in 200 mL of deionized water yielding 0.01 M phosphate buffer, 0.0027 M potassium chloride and 0.137 M sodium chloride at pH 7.4 and at 25 °C. For the spectroscopy experiments, a stock solution was prepared by dissolving the correct amount BTA **1** in methanol to afford solution with a total concentration of 10 mM or 15 mM in MeOH. Subsequently, 3.5 μL of the 10 mM stock solution was injected into 3.5 mL PBS, to give a total BTA concentration of 10 μM in PBS buffer. Alternatively, 10 μL of the 15 mM stock solution was injected into to 3 mL Milli-Q water to afford a 50 μM solution in water. All solutions were first annealed overnight at room temperature and then the UV or CD spectra were measured. For the SAXS and cryo-TEM measurements the samples were prepared as follows. A stock solution of **1** in MeOH was prepared by dissolving the appropriate amount of **1** into a vial. Then, the MeOH was removed under a stream of argon. Subsequently, the sample was placed in a vacuum oven at 40 °C for one hour. Then, 0.5 mL of Milli-Q water was added and the sample was sonicated during two minutes yielding a slightly turbid solution. After equilibration overnight at room temperature, a completely clear solution was obtained. The final concentration of **1** was 4.5 mg mL^{-1} for the SAXS and 0.5 mg mL^{-1} for cryo-TEM measurements.

All ^{1}H-NMR and ^{13}C-NMR spectra were recorded on a Varian Mercury Vx 400 MHz and/or a Varian 400 MHz (400 MHz for ^{1}H-NMR and 100 MHz for ^{13}C-NMR). Proton chemical shifts are reported in ppm (δ) downfield from

trimethylsilane (TMS) using the resonance frequency of the deuterated solvent as the internal standard. Peak multiplicity is abbreviated as s: singlet; d: doublet; t: triplet; q: quartet; sept: septet; m: multiplet; bs: broad singlet; brsept: broad septet. Carbon chemical shifts are reported in ppm (δ) downfield from TMS using the resonance frequency of the deuterated solvent as the internal standard. Matrix assisted laser absorption/ionization mass spectra (MALDI) were obtained on a PerSeptive Biosystems Voyager DE-PRO spectrometer using α-cyano-4-hydroxycinnamic acid (CHCA) or *trans*-2-[3-(4-*tert*-butylphenyl)-2-methyl-2-propenylidene]malononitrile (DCBT) as matrix. Electrospray ionization mass spectra were recorded using a LCQ Fleet (Thermo Finnigan) ion-trap mass spectrometer equipped with a Surveyor autosampler and Surveyor PDA detector (Thermo Finnigan). Solvents were pumped with a flow of 0.2 mL min^{-1} using a high-pressure gradient system using two LC-10AD pumps (Shimadzu). Before mass analysis, the crude was ran over a reverse phase C18 column (GraceSmart 2 × 50 mm, Grace) using a 2–90% acetonitrile linear gradient in water with 0.1% formic acid (FA). Infrared spectra were recorded using a Perkin Elmer Spectrum Two FT-IR spectrometer equipped with a Perkin Elmer Universal ATR Two Accessory. UV-Vis experiments were performed on a Jasco V-650 spectrophotometer equipped with a JASCO ETCR-762 temperature controller or a Varian 300 Bio UV-Visible spectrophotometer equipped with a Varian Carey temperature controller. Circular dichroism measurements were performed with a Jasco J-815 spectropolarimeter in combination with a PFD-425S/15 Peltier-type temperature controller. For all experiments the linear dichroism (LD) was also measured and in all cases no LD was observed. The molar circular dichroism $\Delta\varepsilon$ was calculated from $\Delta\varepsilon$ = CD effect/(32 980 × c × l) in which c is the concentration and l is the optical path length. All spectroscopic experiments were conducted at 20 °C and a quartz cuvette with a 1 cm path length. Small angle X-ray scattering measurements were performed on a SAXSLAB GANESHA 300 XL SAXS system equipped with a GeniX 3D Cu Ultra Low Divergence micro focus sealed tube source producing X-rays with a wavelength λ = 1.54 Å at a flux of 1 × 10^8 ph s^{-1} and a Pilatus 300 K silicon pixel detector with 487 × 619 pixels of 172 μm^2 in size placed at a sample-to-detector distances of 713 to access a q-range of 0.15 ≤ q ≤ 4.39 nm^{-1} with $q = 4\pi/\lambda(\sin\theta/2)$. Silver behenate was used for calibration of the beam centre and the q range. Samples were contained in 2 mm quartz capillaries (Hilgenberg Gmbh, Germany). The two-dimensional SAXS patterns were brought to an absolute intensity scale using the calibrated detector response function, known sample-to-detector distance, measured incident and transmitted beam intensities, and azimuthally averaged to obtain one-dimensional SAXS profiles. The scattering curves of the supramolecular polymers were obtained by subtraction of the scattering contribution of the solvent and quartz cell. Cryogenic transmission electron microscopy was measured on samples with a concentration of 0.5 mg mL^{-1}. Vitrified films were prepared in a 'Vitrobot' instrument at 22 °C and at a humidity of 100%. In the preparation chamber of the 'Vitrobot' a 3 μl sample was applied on a Quantifoil grid (R 2/2, Quantifoil Micro Tools GmbH) which was surface plasma treated just prior to use (Cressington 208 carbon coater operating at 5 mA for 40 s). Excess sample was removed by blotting using filter paper for 3 s at −3 mm and the thin film thus formed was plunged (acceleration about 3 g) into liquid ethane just above its freezing point. The vitrified film was transferred to a cryoholder (Gatan 626) and observed at temperatures below −170 °C in a Tecnai Sphera microscope operating at 200 kV. Micrographs were taken at low dose conditions, with defocus settings of 5 and 10 μm. High performance liquid chromatography (HPLC) analyses were carried out on a Shimadzu SCL-10Avp with UV-diode array and equipped with a Chiralpack-IA-3 column (100 × 2.1 mm, 3 μm) from Daicel.

Synthetic procedures

11-Azidoundecanoic acid (4). 11-Bromoundecanoic acid (2.03 g, 7.65 mmol) and sodium azide (0.813 g, 12.5 mmol) were dissolved in DMSO (70 mL) and stirred overnight at room temperature under an Ar atmosphere. The solution was quenched with 150 mL water. The product was extracted into ether (3 × 200 mL). The ether layers were combined, washed with acidified brine (350 mL), dried with Na_2SO_4 and the solvent was removed *in vacuo.* Yield = 1.52 g, 87%. ^{1}H NMR (400 MHz, $CDCl_3$): δ = 3.26 (t, J^3 = 6.9 Hz, 2H, $N_3CH_2CH_2$), 2.35 (t, J^3 = 7.5 Hz, 2H, CH_2COOH), 1.62 (m, 4H, $CH_2CH_2CH_2COOH$, $CH_2CH_2CH_2COOH$), 1.41–1.25 (m, 12H, aliphatic). ^{13}C NMR (100 MHz, $CDCl_3$) δ = 179.77, 51.48, 33.97, 29.38, 29.28, 29.18, 29.11, 29.01, 28.83, 26.70, 24.65. MALDI-TOF-MS: calcd for $C_{11}H_{21}N_3O_2$ $[M - H]^-$ 226.15, found 226.20. FT-IR (ATR) ν (cm^{-1}): 2929, 2856, 2096, 1709, 1458, 1413, 1349, 1285, 1257, 1103, 936, 723, 640, 553, 485.

(2*S*,4*R*)-Di-*t*-butyl 4-((11-azidoundecanoyl)oxy)pyrrolidine-1,2-dicarboxylate (5). Under an Ar atmosphere, a round bottom flask was charged with 11-azidoundecanoic acid **4** (0.360 g, 1.59 mmol), (2*S*,4*R*)-di-*tert*-butyl 4-hydroxypyrrolidine-1,2-dicarboxylate **3** (0.494 g, 1.72 mmol), 4-(dimethylamino)-pyridinium 4-toluenesulfonate (DPTS) (0.796 g, 2.70 mmol) and dry chloroform (10 mL). The solution was cooled in an ice/salt bath to below 0 °C and a cooled solution of *N*-(3-dimethylaminopropyl)-*N*′-ethylcarbodiimide hydrochloride (0.943 g, 4.92 mmol) in dry chloroform (3 mL) was added quickly. The clear solution was stirred at room temperature overnight. Then, the reaction mixture was transferred to a separatory funnel, additional chloroform was added (30 mL), and the solution was washed with water (2 × 40 mL) and brine (40 mL). The organic layer was dried over $MgSO_4$ and the solvent was removed *in vacuo*. The material was purified by column chromatography (eluent heptane/ethyl acetate 90/10 to 75/25 v/v) yielding the target compound (0.584 g, 74%). ^{1}H NMR (400 MHz, $CDCl_3$): δ = 5.25 (bs, 1H, C═OOC*H*), 4.23 (m, 1H, CH_2CHC═O), 3.66 (m, 2H, $CHCH_2N$), 3.25 (t, J^3 = 6.9 Hz, 2H, N_3CH_2), 2.33 (m, 1H, $CHCH_2CH$), 2.28 (t, J^3 = 7.5 Hz, 2H, CH_2C═O), 2.17 (m, 1H, $CHCH_2CH$), 1.70–1.53 (m, 4H, $CH_2CH_2CH_2C$═O, $CH_2CH_2CH_2C$═O), 1.53–1.39 (m, 18H,

CH_3C), 1.39–1.10 (m, 12H, aliphatic). ^{13}C NMR (100 MHz, $CDCl_3$) δ = 173.23, 171.62, 153.84, 81.39, 80.29, 71.61, 58.49, 51.99, 51.48, 36.70, 34.26, 29.40, 29.30, 29.19, 29.11, 29.05, 28.83, 28.33, 28.01, 27.94, 26.70, 24.82. MALDI-TOF-MS: calcd for $C_{25}H_{44}N_4O_6$ $[M + Na]^+$ 519.32, found 519.31. FT-IR (ATR) ν (cm^{-1}): 2978, 2930, 2857, 2095, 1739, 1705, 1457, 1395, 1367, 1256, 1219, 1153, 1069, 995, 854, 771.

(2*S*,4*R*)-Di-*t*-butyl 4-((11-aminoundecanoyl)oxy)pyrrolidine-1,2-dicarboxylate (6). A 25 mL round bottom flask was charged with **5** (0.541 g, 1.10 mmol), triphenylphosphine (570 mg, 2.17 mmol, 1.99 eq.) and THF (8 mL). The solution was stirred at 35 °C overnight. A mixture of water (2.4 mL) and THF (1.6 mL) was added and stirring was continued at 35 °C overnight. The volatiles were removed *in vacuo* and the remaining water was removed on the freeze dryer. The crude was concentrated *in vacuo* and purified by column chromatography (eluent chloroform/methanol/triethylamine 100/0/0 to 91/7/2 v/v/v). Yield = 0.226 g, 44%. Oligomerisation of **6** yields amide oligomers (~20% impurity, based on LC-MS), which were not removed at this stage. ^1H NMR (400 MHz, $CDCl_3$): δ = 5.25 (bs, 1H, C═OOC*H*), 4.25 (m, 1H, CH_2CHC═O), 3.72–3.45 (m, 2H, $CHCH_2N$), 2.67 (t, J^3 = 6.9 Hz, 2H, H_2NCH_2), 2.34 (m, 1H, $CHCH_2CH$), 2.28 (t, J^3 = 7.6 Hz, 2H, CH_2C═O), 2.16 (m, 1H, $CHCH_2CH$), 1.65–1.54 (m, 2H, CH_2CH_2C═O), 1.50–1.38 (m, 18H, CCH_3), 1.37–1.20 (m, 14H, aliphatic). ^{13}C NMR (100 MHz, $CDCl_3$) δ = 173.25, 171.62, 81.40, 80.29, 77.33, 77.22, 77.01, 76.70, 71.60, 58.49, 51.99, 42.25, 36.70, 34.27, 33.80, 29.55, 29.46, 29.38, 29.22, 29.07, 28.33, 28.01, 26.88, 24.84. MALDI-TOF: calcd for $C_{25}H_{46}N_2O_6$ $[M + Na]^+$ 493.34, found 493.33. FT-IR (ATR) ν (cm^{-1}): 3314, 2977, 2927, 2854, 1740, 1705, 1560, 1458, 1397, 1367, 1256, 1220, 1160, 1068, 995, 937, 854, 771, 555.

(2*S*,4*R*)-Di-*tert*-butyl 4-((11-(3,5-bis((1-hydroxy-3,6,9,12-tetraoxatetracosan-24-yl)carbamoyl)benzamido)undecanoyl)oxy)-pyrrolidine-1,2-dicarboxylate (8). 3,5-Bis((1-hydroxy-3,6,9,12-tetraoxatetracosan-24-yl)carbamoyl)benzoic acid **7** (0.100 g, 1.08 mmol) and the reduced, proline functionalised spacer **6** (55.9 mg, 1.19 mmol, 1.1 eq.) were dissolved in DMF (1 mL). DMT-MM (70 mg, 0.253 mmol, 2.4 eq.) was added and the mixture was stirred at room temperature overnight. Then, chloroform (5 mL) was added and the solution was transferred to a separatory funnel. The organic layer was washed with water (2 × 5 mL) and brine (5 mL) and dried over $MgSO_4$. The solvent was removed *in vacuo* and the crude was purified by reverse phase column chromatography (acetonitrile/water/THF 67/33/0 to 60/20/20 v/v/v). Yield = 51.8 mg (34.8%). The coupling of **6** to the BTA yields a ~20% impurity (based on LC-MS). ^1H NMR (400 MHz, $CDCl_3$): δ = 8.36 (m, 3H, Ar), 6.72–6.54 (m, 3H, C═ON*H*CH_2), 5.25 (bs, 1H, C═OOC*H*), 4.25 (m, 1H, CH_2CHC═O), 3.75–3.54 (m, 34H, O–$(CH_2)_2$–O), $CHCH_2N$, 3.51–3.38 (m, 10H, CH_2CH_2NHC═O, $CH_2CH_2CH_2O$), 2.78 (bs, 2H, CH_2OH), 2.40–2.25 (m, 3H, CH_2CH_2C═O, $CHCH_2CH$), 2.21–2.10 (m, 1H, $CHCH_2CH$), 1.74–1.51 (m, 10H, $CH_2CH_2CH_2O$, $CH_2CH_2CH_2O$, CH_2CH_2C═O), 1.49–1.41 (m, 18H, CCH_3), 1.41–1.20 (m, 46H, aliphatic). ^{13}C NMR (100 MHz, $CDCl_3$) δ = 165.69, 135.27, 110.01, 77.33, 77.33, 77.01, 77.01, 76.69, 76.69, 72.54, 72.54, 71.55, 70.62, 70.62, 70.56, 70.56, 70.33, 70.33, 70.02, 61.72, 51.98, 40.37, 29.55, 29.55, 29.49, 29.44, 29.39, 29.20, 29.03, 28.38, 28.33, 28.02, 27.94, 26.92, 26.03, 26.03. ESI MS: calcd for $C_{74}H_{132}N_4O_{19}$ $[M + Na]^+$ 1403.94, found 1404.08. FT-IR (ATR) ν (cm^{-1}): 3335, 3074, 2926, 2855, 1740, 1706, 1649, 1537, 1458, 1399, 1367, 1288, 1259, 1149, 1125, 942, 842, 772, 707, 555.

(2*S*,4*R*)-4-((11-(3,5-Bis((1-hydroxy-3,6,9,12-tetraoxatetracosan-24-yl)carbamoyl)benzamido)undecanoyl)oxy)pyrrolidine-2-carboxylic acid (1). Under an Ar atmosphere, the functionalized BTA **8** (293 mg, 0.212 mmol) was dissolved in 1 : 1 dichloromethane : trifluoroacetic acid (4 mL) and stirred overnight at room temperature. The volatiles were removed under a nitrogen stream, water (2 mL) was added and the solution was stirred overnight. The water was removed on the freeze dryer and the crude was purified by reverse phase column chromatography (water/acetonitrile 50/50 to 30/70 v/v) yielding **1** as a sticky, white solid (182 mg, 70%). ^1H NMR (400 MHz, $CDCl_3$): δ = 8.39 (m, 3H, Ar), 7.61 (bs, 1H, C═ON*H*CH_2), 7.49 (bs, 2H, C═ON*H*CH_2), 5.34 (bs, 1H, C═OOC*H*), 5.13 (m, 1H, $CH_2CHCOOH$), 4.36 (m, 2H, $CHCH_2NH$), 3.76–3.53 (m, 32H, O–$(CH_2)_2$–O), 3.49–3.28 (m, 10H, CH_2CH_2NHC═O, $CH_2CH_2CH_2O$), 2.50–2.24 (m, 4H, CH_2CH_2C═O, $CHCH_2CH$), 1.65–1.41 (m, 10H, $CH_2CH_2CH_2O$, $CH_2CH_2CH_2O$, CH_2CH_2-C═O), 1.39–1.18 (m, 46H, aliphatic). ^{13}C NMR (100 MHz, $CDCl_3$) δ = 172.99, 166.72, 134.94, 128.70, 75.60, 72.42, 71.51, 70.29, 70.43, 70.03, 69.82, 61.37, 40.48, 33.81, 29.47, 29.40, 29.35, 29.24, 28.99, 28.79, 28.70, 26.97, 26.78, 25.95, 24.45. ESI MS: calcd for $C_{65}H_{116}N_4O_{17}$ $[M + H]^+$ 1225.83, found 1226.17. FT-IR (ATR) ν (cm^{-1}): 3320, 3073, 2925, 2855, 1740, 1648, 1545, 1456, 1349, 1290, 1200, 1131, 940, 831, 799, 720.

Conclusions

Attaching an L-Pro unit covalently to a water-compatible benzene-1,3,5-tricarboxamide affords one-dimensional, helical supramolecular polymers that are catalytically active in water. The formed supramolecular polymers have a cross-section <10 nm and lengths in the micrometre range. At higher concentrations, the supramolecular polymers start to interact, resulting in an increase in the viscosity of the solutions. Evaluation of the catalytic activity of these supramolecular polymers reveals high activity and selectivity for aldol reactions in water with the reactive substrate pair *p*-nitrobenzaldehyde and cyclohexanone. At catalysts concentrations of 1 mol%, full conversion is achieved within 24 h and de_{anti} and ee_{anti} are as high as 93 and 98%, respectively. Mixing of the organocatalyst with catalytically inactive BTAs results in a system of similar activity and selectivity, suggesting that the environment around the L-Pro unit remains the same. Furthermore, the catalytic behaviour of this supramolecular polymer is highly reproducible and the catalyst can be reused.

Many molecular and macromolecular organocatalysts have been reported nowadays that show excellent activity and

selectivity in water, most of them relying on hydrophobic interactions to create hydrophobic sites for catalysis to take place. Nevertheless, the combination of small, well-defined amphiphilic moieties that polymerise non-covalently in water as a result of directional, supramolecular interactions with (organo)catalytic units opens up novel possibilities for controlled spatial modulation between catalytic sites. Depending on the reaction of interest, this modulation may be crucial to enhance the activity and selectivity. In addition, the supramolecular interactions that stabilise the formed aggregates also allow easy mixing of building blocks with different functions at the periphery. Combining supramolecular (organo)catalysis in water with straightforward separations of the reaction products from the catalysts may open up enzyme-like catalysis for a wide range of non-natural substrates.

Acknowledgements

The authors like to thank Bas van Genabeek for discussions and help with the initial catalysis experiments. This work was financed by the Dutch Ministry of Education, Culture and Science (Gravity program 024.001.035) and the European Research Council (FP7/2007–2013, ERC Grant Agreement 246829). I.K.V. is grateful for financial support from The Netherlands Organisation for Scientific research (NWO – VENI grant: 700.10.406) and the European Union through the Marie Curie 5 Fellowship program FP7-PEOPLE-2011-CIG (contract no. 293788). The ICMS Animation Studio (Eindhoven University of Technology) is acknowledged for providing the TOC image.

Notes and references

1 (*a*) D. E. Bergbreiter, J. Tian and C. Hongfa, *Chem. Rev.*, 2009, **109**, 530–582; (*b*) J. Lu and P. H. Toy, *Chem. Rev.*, 2009, **109**, 815–838; (*c*) D. E. Bergbreiter, *ACS Macro Lett.*, 2014, **3**, 260–265.

2 B. Escuder, F. Rodrigues-Llansola and J. F. Miravet, *New J. Chem.*, 2010, **34**, 1044–1054.

3 M. O. Guler and S. I. Stupp, *J. Am. Chem. Soc.*, 2007, **129**, 12082–12083.

4 M. Raynal, F. Portier, P. W. N. M. van Leeuwen and L. Bouteiller, *J. Am. Chem. Soc.*, 2013, **135**, 17687–17690.

5 (*a*) C. Zhang, X. Xue, Q. Luo, Y. Li, K. Yang, X. Zhuang, Y. Jiang, J. Zhang, J. Liu, G. Zou and X.-J. Liang, *ACS Nano.*, 2014, **8**, 11715–11723; (*b*) F. Rodriguez-Llansola, B. Escuder and J. F. Miravet, *Org. Biomol. Chem.*, 2009, **7**, 3091–3094.

6 (*a*) B. List, *Tetrahedron*, 2002, **58**, 5572–5590; (*b*) N. Mase and C. F. Barbas III, *Org. Biomol. Chem.*, 2010, **8**, 4043–4050; (*c*) P. M. Pihko, I. Majander and A. Erkkilä, *Top. Curr. Chem.*, 2010, **291**, 29–75.

7 A. Córdova, W. Notz and C. F. Barbas III, *Chem. Commun.*, 2002, 3024–3025.

8 (*a*) Y. Hayashi, T. Sumiya, J. Takahashi, H. Gotoh, T. Urushima and M. Shoji, *Angew. Chem., Int. Ed.*, 2006, **45**, 958–961; (*b*) Y. Hayashi, S. Aratake, T. Okano, J. Takahashi, T. Sumiya and M. Shoji, *Angew. Chem., Int. Ed.*, 2006, **45**, 5527–5529.

9 L-Proline, when properly modified, exhibits good activity and selectivity in aqueous environment. (*a*) M. Raj and V. K. Singh, *Chem. Commun.*, 2009, 6687–6703; (*b*) J. Mlynarski and S. Bas, *Chem. Soc. Rev.*, 2014, **43**, 577–587; (*c*) A. S. Kucherenko, D. E. Siyutkin, R. R. Dashkin and S. G. Zlotin, *Russ. Chem. Bull.*, 2013, **62**, 1010–1015.

10 E. Huerta, B. van Genabeek, B. A. G. Lamers, M. M. E. Koenigs, E. W. Meijer and A. R. A. Palmans, *Chem. – Eur. J.*, 2015, **21**, 3682–3690.

11 C. M. A. Leenders, L. Albertazzi, T. Mes, M. M. E. Koenigs, A. R. A. Palmans and E. W. Meijer, *Chem. Commun.*, 2013, **49**, 1963–1965.

12 E. Huerta, B. van Genabeek, P. J. M. Stals, E. W. Meijer and A. R. A. Palmans, *Macromol. Rapid Commun.*, 2014, **35**, 1320–1325.

13 L. Albertazzi, D. van der Zwaag, C. M. A. Leenders, R. Fitzner, R. W. van der Hofstad and E. W. Meijer, *Science*, 2014, **344**, 491–495.

14 D. R. Lide, *CRC Handbook of Chemistry and Physics*, CRC Press, 84th edn, 2003.

15 (*a*) P. Besenius, G. Portale, H. M. Janssen, A. R. A. Palmans and E. W. Meijer, *Proc. Natl. Acad. Sci. U. S. A.*, 2010, **107**, 17888–17893; (*b*) I. de Feijter, P. Besenius, L. Albertazzi, E. W. Meijer, A. R. A. Palmans and I. K. Voets, *Soft Matter*, 2013, **9**, 10025–10030.

16 M. M. J. Smulders, A. P. H. J. Schenning and E. W. Meijer, *J. Am. Chem. Soc.*, 2008, **130**, 606–611.

17 M. B. Baker, L. Albertazzi, I. K. Voets, C. M. A. Leenders, A. R. A. Palmans, G. M. Pavan and E. W. Meijer, *Nat. Commun.*, 2015, **6**, 6234.

18 Y. Nakano, T. Hirose, P. J. M. Stals, E. W. Meijer and A. R. A. Palmans, *Chem. Sci.*, 2012, **3**, 148–155.

19 J. S. Pedersen and P. Schurtenberger, *Macromolecules*, 1996, **29**, 7602–7612.

20 (*a*) E. G. Doyagüez, G. Corrales, L. Garrido, J. Rodríguez-Hernández, A. Gallardo and A. Fernández-Mayoralas, *Macromolecules*, 2011, **44**, 6269–6276; (*b*) E. G. Doyagüez, J. Rodríguez-Hernández, G. Corrales, A. Fernández-Mayoralas and A. Gallardo, *Macromolecules*, 2012, **45**, 7676–7683; (*c*) Q. Zha, Y.-H. Lam, M. Kheirabadi, C. Xu, K. N. Houk and C. E. Schafmeister, *J. Org. Chem.*, 2012, **77**, 4784–4792; (*d*) C. Berdugo, J. F. Miravet and B. Escuder, *Chem. Commun.*, 2013, **49**, 10608–10610; (*e*) Z. An, Y. Guo, L. Zhao, Z. Li and J. He, *ACS Catal.*, 2014, **4**, 2566–2576.

21 (*a*) S. Bahmanyar, K. N. Houk, H. J. Martin and B. List, *J. Am. Chem. Soc.*, 2003, **125**, 2475–2479; (*b*) K. Sakthivel, W. Notz, T. Bui and C. F. Barbas III, *J. Am. Chem. Soc.*, 2001, **123**, 5260–5267.

22 (*a*) F. Giacalone, M. Gruttadauria, P. Agrigento and R. Noto, *Chem. Soc. Rev.*, 2012, **41**, 2406–2447; (*b*) F. Giacalone,

M. Gruttadauria, P. Agrigento, P. Lo Meo and R. Noto, *Eur. J. Org. Chem.*, 2010, 5696–5704.

23 B. H. Lipshutz and S. Ghorai, *Org. Lett.*, 2012, **14**, 422–425.

24 (*a*) A. Lu, P. Cotanda, J. P. Patterson, D. A. Longbottom and R. K. O'Reilly, *Chem. Commun.*, 2012, **48**, 9699–9701; (*b*) A. Lu, D. Moatsou, D. A. Longbottom and R. K. O'Reilley, *ACS Macro Lett.*, 2014, **3**, 1235–1239; (*c*) H. A. Zayas, A. Lu, D. Valade, F. Amir, Z. Jia, R. K. O'Reilly and M. J. Monteiro, *ACS Macro Lett.*, 2013, **2**, 327–331; (*d*) A. Lu, D. Moatsou, D. A. Longbottom and R. K. O'Reilly, *Chem. Sci.*, 2013, **4**, 965–969.

25 L-Proline attached to poly(ethylene oxide) have been evaluated in polar aprotic solvents, in which good yields and selectivities for the aldol reaction were observed. See: (*a*) M. Benaglia, G. Celentano and F. Cozzi, *Adv. Synth. Catal.*, 2001, **343**, 171–173; (*b*) M. Benaglia, M. Cinquini, F. Cozzi, A. Puglisi and G. Celentano, *Adv. Synth. Catal.*, 2002, **344**, 533–542.

26 D. Font, S. Sayalerno, A. Bastero, C. Jimeno and M. A. Pericas, *Org. Lett.*, 2008, **10**, 337–340.

27 E. Huerta, P. J. M. Stals, E. W. Meijer and A. R. A. Palmans, *Angew. Chem., Int. Ed.*, 2013, **52**, 2906–2910.

28 The UV spectra of **1** and **2** are identical making it impossible to distinguish between a random mixture of the two BTAs within one supramolecular polymer or a mixture of two different of supramolecular polymers. Characterisation of the mixture of **1** and **2** at the condition in which catalysis was performed also showed a UV trace identical to those of pure **1** and **2**.

29 L. Albertazzi, F. J. Martinez-Veracoecheab, C. M. A. Leenders, I. K. Voets, D. Frenkel and E. W. Meijer, *Proc. Natl. Acad. Sci. U. S. A.*, 2013, **110**, 12203–12208.

30 Organocatalysts in which directional hydrogen bonding interactions are important to achieve active catalysts have been investigated. (*a*) J. P. Delaney and L. C. Henderson, *Adv. Synth. Catal.*, 2012, **354**, 197–204; (*b*) M. Shao, Q. Jin, L. Zhang and M. Liu, *Chem. Lett.*, 2012, **41**, 1349–1350; (*c*) F. Rodríguez-Llansola, B. Escuder and J. F. Miravet, *Chem. Commun.*, 2009, 7303–7305.

31 A. M. P. Koskenen, J. Helaja, E. T. T. Kumpulainen, J. Koivisto, H. Mansikkamäki and K. Rissanen, *J. Org. Chem.*, 2005, **70**, 6447–6453.

32 (*a*) M. Kunishima, C. Kawachi, J. Monta, K. Terao, F. Iwasaki and S. Tani, *Tetrahedron*, 1999, **55**, 13159–13170; (*b*) Z. J. Kamiński, P. Paneth and J. Rudziński, *J. Org. Chem.*, 1998, **63**, 4248–4255.